

# A Review: Synthesis and Applications of Titanium Sub-Oxides

Xiaoping Wu <sup>1,\*</sup> , Haibo Wang <sup>1</sup> and Yu Wang <sup>2</sup>

<sup>1</sup> State Key Laboratory of V and Ti Resources Comprehensive Utilization, Ansteel Research Institute of Vanadium & Titanium (Iron & Steele), Panzhihua 617000, China; 15273187604@163.com

<sup>2</sup> The School of Chemistry and Chemical Engineering, State Key Laboratory of Power Transmission Equipment & System Security and New Technology, Chongqing University, 174 Shazheng Street, Shapingba District, Chongqing 400044, China; wangy@cqu.edu.cn

\* Correspondence: 13308173290@163.com

**Abstract:** Magnéli phase titanium oxides, also called titanium sub-oxides ( $\text{Ti}_n\text{O}_{2n-1}$ ,  $4 < n < 9$ ), are a series of electrically conducting ceramic materials. The synthesis and applications of these materials have recently attracted tremendous attention because of their applications in a number of existing and emerging areas. Titanium sub-oxides are generally synthesized through the reduction of titanium dioxide using hydrogen, carbon, metals or metal hydrides as reduction agents. More recently, the synthesis of nanostructured titanium sub-oxides has been making progress through optimizing thermal reduction processes or using new titanium-containing precursors. Titanium sub-oxides have attractive properties such as electrical conductivity, corrosion resistance and optical properties. Titanium sub-oxides have played important roles in a number of areas such as conducting materials, fuel cells and organic degradation. Titanium sub-oxides also show promising applications in batteries, solar energy, coatings and electronic and optoelectronic devices. Titanium sub-oxides are expected to become more important materials in the future. In this review, the recent progress in the synthesis methods and applications of titanium sub-oxides in the existing and emerging areas are reviewed.

**Keywords:** synthesis; application; titanium sub-oxides; Magnéli phase



**Citation:** Wu, X.; Wang, H.; Wang, Y. A Review: Synthesis and Applications of Titanium Sub-Oxides. *Materials* **2023**, *16*, 6874. <https://doi.org/10.3390/ma16216874>

Academic Editor: Aivaras Kareiva

Received: 10 September 2023

Revised: 16 October 2023

Accepted: 20 October 2023

Published: 26 October 2023



**Copyright:** © 2023 by the authors. Licensee MDPI, Basel, Switzerland. This article is an open access article distributed under the terms and conditions of the Creative Commons Attribution (CC BY) license (<https://creativecommons.org/licenses/by/4.0/>).

## 1. Introduction

Titanium sub-oxides, often referred to as Magnéli phase  $\text{TiO}_x$ , comprise a series of different titanium oxides that have the general formula  $\text{Ti}_n\text{O}_{2n-1}$  ( $4 \leq n \leq 10$ ) [1–5]. It is well-known that titanium dioxide ( $\text{TiO}_2$ ) is an electrical insulator, as it has a large band gap (anatase: 3.2 eV; 3.0: rutile) [6]. However, Magnéli phase titanium oxides are electrically conducting, and the value of electrical resistivity decreases with the increase in the oxygen deficiency [7]. Furthermore, Magnéli phase  $\text{TiO}_x$  are found to be more stable than carbon in electrochemically oxidizing conditions [1,8]. These titanium sub-oxides have attracted much recent attention as promising new conducting materials because they are electrically conducting, and are highly stable towards chemical corrosion.

The earliest phase analysis using X-ray methods on the oxygen–titanium system was carried out by Ehrlich, who reported the existence of three intermediary titanium oxides [9,10]. In the 1950s, a phase diagram of a titanium–oxygen system was constructed from data in the literature by DeVries et al. [11]; later, a comprehensive phase analysis of  $\text{TiO}_x$  was studied by the group of Arne Magnéli, and a number of phases in the titanium–oxygen system were reported, including  $\text{Ti}_4\text{O}_7$ ,  $\text{Ti}_5\text{O}_9$ ,  $\text{Ti}_6\text{O}_{11}$ ,  $\text{Ti}_7\text{O}_{13}$ ,  $\text{Ti}_8\text{O}_{15}$ ,  $\text{Ti}_9\text{O}_{17}$  and  $\text{Ti}_{10}\text{O}_{19}$  [12]. The electrical properties of these titanium oxides were studied by Bartholomew et al., and it was found that titanium sub-oxides have semiconductor-to-metal transitions at certain temperatures and their electrical conductivities change with the oxygen content of those materials [13].  $\text{Ti}_4\text{O}_7$  has the highest electrical conductivity among Magnéli phase  $\text{TiO}_x$  at room temperature [1].

Magnéli phase  $\text{TiO}_x$  are generally synthesized by the reduction of  $\text{TiO}_2$ . The reduction sequence is as follows:  $\text{TiO}_2 \rightarrow \text{Ti}_n\text{O}_{2n-1}$  ( $n > 10$ )  $\rightarrow \text{Ti}_n\text{O}_{2n-1}$  ( $4 < n < 10$ )  $\rightarrow \text{Ti}_3\text{O}_5 \rightarrow \text{Ti}_2\text{O}_3 \rightarrow \text{TiO} \rightarrow \text{Ti}_2\text{O}$  [14]. Oxygen defect formations and its concentration depend on the synthesis conditions.  $\text{Ti}_4\text{O}_7$  can be expressed as  $\text{TiO}_{1.75}$ , as the ratio of O/Ti of  $\text{Ti}_4\text{O}_7$  is 1.75. The Magnéli phase  $\text{Ti}_n\text{O}_{2n-1}$  are the intermediate products. It is critical to have well-controlled preparation conditions to synthesize each Magnéli phase, with high chemical and phase purities that have significant effects on the intrinsic properties such as electrical, optical behavior and their catalytic activity.

It is increasingly important to synthesize nanostructured titanium sub-oxides because of their particular properties resulting from the high surface areas of the materials [15–18]. Progress has been made in applying nanostructured titanium sub-oxides in the areas of fuel cells, water treatment, batteries and so on. To update the recent research progress of synthesis and applications of titanium sub-oxides, this review will discuss and highlight the recent developments in the synthesis and applications of  $\text{Ti}_4\text{O}_7$  in the fields of energy, environment, catalysts and others, as well as future directions for research.

## 2. Synthesis Methods

The phase diagram of the Ti–O system (Figure 1) shows various stable phases at different O/Ti ratios. The region at the right of the diagram contains the discrete Magnéli phases of  $\text{Ti}_n\text{O}_{2n-1}$  ( $n = 4-10$ ) and  $\text{TiO}_2$ . At sufficiently elevated temperatures,  $\text{TiO}_2$  can be reduced to a lower oxidation state such as Magnéli series, including  $\text{Ti}_4\text{O}_7$ . To obtain individual phases such as  $\text{Ti}_4\text{O}_7$  in the Magnéli series, the condition for reduction of  $\text{TiO}_2$  needs to be carefully controlled. The key parameters for the synthesis of  $\text{Ti}_4\text{O}_7$ , as well as for other Magnéli phases, include temperature, time, reducing atmosphere and reducing agents. Hydrogen, carbon, metal and hydride can be used as reducing agents.

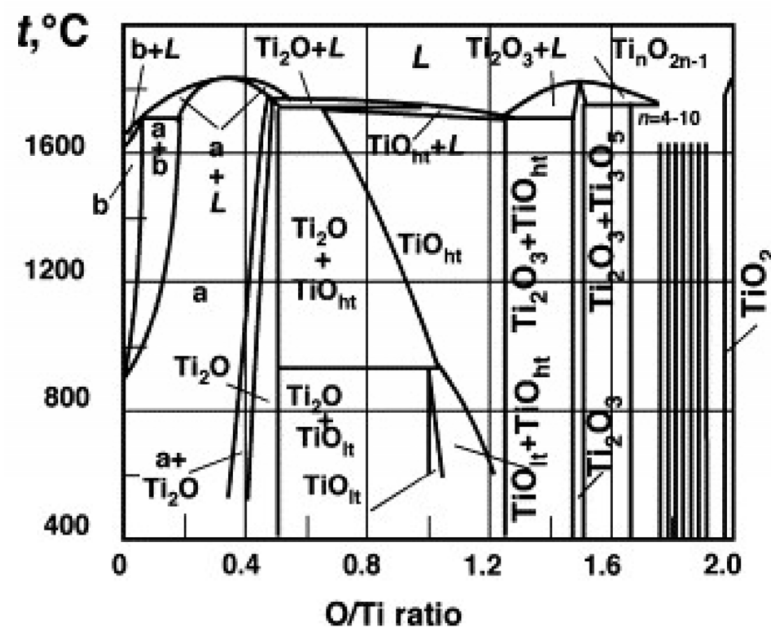


**Figure 1.** Phase diagram of the Ti–O system (Reprinted from ref. [14], copyright 2018, MDPI).

### 2.1. Reduction of $\text{TiO}_2$ by Hydrogen

At sufficiently elevated temperatures, hydrogen ( $\text{H}_2$ ) or a mixture hydrogen–inert gas such as argon (Ar) is used to reduce  $\text{TiO}_2$  into the titanium sub-oxides [1]. The reduction process can be considered to be a reaction of oxygen being removed progressively from  $\text{TiO}_2$ . The reaction for the synthesis of  $\text{Ti}_4\text{O}_7$  through hydrogen reduction is shown in Equation (1):



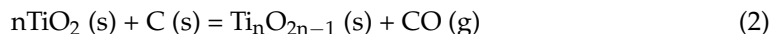
The reduction reaction to produce  $Ti_4O_7$  is carried out at sufficiently elevated temperature, generally higher than 1000 °C. The sequence of the formation of Magnéli series  $TiO_x$  in the hydrogen reduction reactions of  $TiO_2$  is  $Ti_9O_{17}$ ,  $Ti_8O_{15}$ ,  $Ti_7O_{13}$ ,  $Ti_6O_{11}$ ,  $Ti_5O_9$  and  $Ti_4O_7$ . The reduction reaction of  $TiO_2$  is carried out in a flow of hydrogen in a reactor that is heated externally to maintain a high temperature. As  $Ti_4O_7$  is the last in the reduction sequence, the synthesis of  $Ti_4O_7$  needs higher temperature, longer reduction time or a combination of two, compared with the parameters to the formation of other Magnéli series. The reaction temperature, reaction time, gas composition and size of  $TiO_2$  particles are important factors for the synthesis of Magnéli phases [2,3]. A summary of the synthesis of  $Ti_4O_7$  through hydrogen reduction can be found in Table 1.

**Table 1.** Summary of synthesis of  $Ti_4O_7$  and other titanium sub-oxides.

Synthesis Method	Process Conditions	Characterization	Ref.
H <sub>2</sub> reduction	Pigmentary $TiO_2$ reacts with H <sub>2</sub> at 1050 °C	Monophasic $Ti_4O_7$	[4]
H <sub>2</sub> reduction	Anatase $TiO_2$ reacts with H <sub>2</sub> (99.99%) at 950 °C	Pure triclinic phase of $Ti_4O_7$ , 0.5–1 μm	[2]
H <sub>2</sub> reduction	$TiO_2$ nanotube arrays react with H <sub>2</sub> at 850 °C for two hours	$Ti_4O_7$ nanotube arrays	[19]
H <sub>2</sub> reduction	$TiO_2$ reacts with H <sub>2</sub>	70% $Ti_4O_7$ , 30% $Ti_5O_9$	[20]
H <sub>2</sub> reduction	Rutile $TiO_2$ was reduced in a mixture of N <sub>2</sub> and H <sub>2</sub> gases	$Ti_4O_7$ , $Ti_5O_9$ and $Ti_6O_{11}$	[21]
H <sub>2</sub> reduction	$TiO(NO_3)_2$ reacts with H <sub>2</sub> at 1000 °C for 6 h	$Ti_4O_7$ , 250 nm	[22]
H <sub>2</sub> reduction	H <sub>2</sub> $TiO_3$ reacts with H <sub>2</sub> /Ar in a thermal plasma reactor	$Ti_nO_{2n-1}$ nanoparticles, 20–100 nm	[23]
H <sub>2</sub> reduction	$TiO_2$ + H <sub>2</sub> in a combined catalytic and thermal reduction reaction	$Ti_8O_{15}$ , $Ti_4O_7$ , $Ti_3O_5$	[24]
C reduction	The reduction of $TiO_2$ by graphite or metallic titanium	Various phases	[25]
C reduction	$TiO_2$ anatase (100 nm) reacts with carbon black at 1020 °C for 0.5–2 h	$Ti_4O_7$ , 98.5%	[26]
C reduction	$TiO_2$ reacts with poly(vinyl alcohol) at 1100 °C	$Ti_4O_7$ , a few hundreds of nm in size	[27]
C reduction	$TiO_2$ reacts with polymer PVP at 925 °C in a microwave furnace	$Ti_4O_7$ nanoparticles (25, 60, and 125 nm)	[28]
C reduction	Reduction of rutile $TiO_2$ in a carbon black micro-environment	Titanium sub-oxide fibers	[29]
Metal reduction	Heating Ti and $TiO_2$ in an electric arc furnace	Titanium sub-oxides	[12]
Metal reduction	Heating $TiO_2$ and Ti metal in an evacuated silica tube at 1150 °C	$Ti_4O_7$ crystals	[30]
Metal reduction	Heating Ti and $TiO_2$ in H <sub>2</sub>	$Ti_4O_7$	[31]
Metal reduction	Heating $TiO_2$ and silicon powder or silicon/ $CaCl_2$ powder	Various titanium sub-oxide powders	[32]
Metal reduction	Reducing macroporous anatase $TiO_2$ using a zirconium getter	$Ti_nO_{2n-1}$ (n = 2, 3, 4, 6)	[33]
Hydride reduction	Solid-phase reaction of $TiO_2$ with $TiH_2$ at relatively low temperature	Titanium sub-oxide nanoparticles	[34]
Hydride reduction	Heating $TiO_2$ nanoparticles and $CaH_2$ powder at 350 °C	$Ti_2O_3$ nanoparticles	[35]
Hydride reduction	$TiO_2$ was embedded with $CaH_2$ and heated at 360 to 500 °C.	$TiO_x$ thin films	[36]

## 2.2. Reduction by Carbon

Titanium dioxide can be reduced by carbon in an inert atmosphere to produce various titanium sub-oxides, as shown in Equation (2):

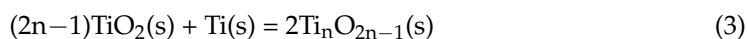


The carbothermal reduction of  $\text{TiO}_2$  is a complex process in which the oxygen in  $\text{TiO}_2$  is progressively removed by carbon.  $\text{TiO}_2$  is initially reduced to  $\text{Ti}_n\text{O}_{2n-1}$ ,  $\text{Ti}_3\text{O}_5$ ,  $\text{Ti}_2\text{O}_3$  and  $\text{TiC}_x\text{O}_y$  [25,37–39], but an over stoichiometric carbon/ $\text{TiO}_2$  ratio may lead to the formation of  $\text{TiC}_x\text{O}_y$ , not titanium sub-oxides.  $\text{Ti}_n\text{O}_{2n-1}$  phases are only formed as intermediates [25,37]. To prepare titanium sub-oxides through the carbothermal reduction of  $\text{TiO}_2$ , the stoichiometric carbon/ $\text{TiO}_2$  ratio is important for the control of the phases formed. The carbothermal reduction of  $\text{TiO}_2$  can be carried out in different gas atmospheres or in a vacuum. Li et al. synthesized  $\text{Ti}_4\text{O}_7$  by reacting  $\text{TiO}_2$  anatase (100 nm) with carbon black at 1020 °C for 0.5–2 h in argon and in a vacuum [26]. The study indicated that at the same temperature, the extent of carbothermal reduction of titanium dioxide is dependent on the molar ratio of  $\text{TiO}_2/\text{C}$ , and excessive carbon may lead to over reduction down the sequence of titanium sub-oxides.  $\text{Ti}_4\text{O}_7$  with a purity of 98.5% was obtained in argon at 1100 °C. Dewan et al. studied the carbothermal reduction of  $\text{TiO}_2$  in hydrogen, helium and argon through temperature-programmed reduction experiments [40]. In argon and helium, the carbothermal reduction of  $\text{TiO}_2$  started at 850 °C. In hydrogen, they found that the phases in a sample after being reduced to 915 °C were  $\text{Ti}_8\text{O}_{15}$  and unreacted  $\text{TiO}_2$ , and the phase in a sample after being reduced to 975 °C was only  $\text{Ti}_4\text{O}_7$ .  $\text{Ti}_4\text{O}_7$  and  $\text{Ti}_3\text{O}_5$  phases were found at 1035 °C.

Titanium sub-oxide fibers with high electrical conductivity have been prepared by reducing  $\text{TiO}_2$  in a carbon black micro-environment [29]. Organic polymers or compounds can be used to synthesize titanium sub-oxides. The carbon in the organic polymers is used as a carbon source for reducing  $\text{TiO}_2$  or other titanium-containing compounds. These organic polymers or compounds include poly (ethyleneimine), polyethyleneglycol [41], poly (styrene-*b*-2-vinylpyridine) [42], resol [43], glucose [44] and poly (vinyl alcohol) [27]. A summary of the various preparation methods for titanium sub-oxides using the carbon reduction method can be found in Table 1.

## 2.3. Reduction by Metals

Metals can be used to reduce  $\text{TiO}_2$  to form titanium sub-oxides [31,32]. Calcium, aluminum, sodium, silicon and titanium have been used to reduce  $\text{TiO}_2$ . For example, by controlling the ratio of metallic titanium and  $\text{TiO}_2$ , metallic titanium (Ti) can be used to reduce  $\text{TiO}_2$  to obtain various titanium sub-oxides through a reaction shown in Equation (3).



Andersson et al. synthesized various titanium sub-oxides by the reduction of  $\text{TiO}_2$  with titanium metal under argon, and established the different phases from X-ray diffraction determinations [9]. Strobel et al. used Ti and  $\text{TiO}_2$  to react in situ in carefully out-gassed transport tubes.  $\text{Cl}_2$  and tellurium tetrachloride were used as transporting agents to synthesize crystals of  $\text{Ti}_n\text{O}_{2n-1}$  with  $n = 2$  to 9 [45]. Gusev et al. developed a method for the synthesis of titanium sub-oxides by reducing  $\text{TiO}_2$  with titanium. This method involved the mechanical activation and annealing in argon at temperatures of 1333–1353 K for 4 h [46]. It is worth noting that the synthesis of titanium sub-oxides using  $\text{TiO}_2$  and Ti can be viewed to be an oxidation reaction in which Ti is oxidized by  $\text{TiO}_2$ . Theoretically, oxidation of Ti is one of the possible ways to obtain titanium suboxides. However, oxygen is highly reactive and can oxidize Ti directly to  $\text{TiO}_2$  easily. Fine Ti powder is far more difficult to prepare than  $\text{TiO}_2$ . A summary of the synthesis of titanium sub-oxides by metal reduction can be found in Table 1.

#### 2.4. Reduction by Hydride

Metal hydrides have strong reducing reactivity, even at low temperatures. The reduction of  $\text{TiO}_2$  to titanium sub-oxides could occur at low temperatures to avoid significant sintering and crystal growth of particles in the formation process of titanium sub-oxides. Therefore, metal hydrides could be used to synthesize nanostructured titanium sub-oxides using nanostructured  $\text{TiO}_2$  as a starting material. Nagao et al. synthesized titanium sub-oxides by reacting  $\text{TiO}_2$  with  $\text{TiH}_2$  at  $550\text{ }^\circ\text{C}$  [34]. The nanoparticles of a series of phases of titanium sub-oxide including  $\text{Ti}_2\text{O}_3$ ,  $\text{Ti}_3\text{O}_5$ ,  $\text{Ti}_4\text{O}_7$  and  $\text{Ti}_8\text{O}_{15}$  were obtained by changing the molar ratios of  $\text{TiO}_2/\text{TiH}_2$ . Other hydride reduction methods for titanium sub-oxide synthesis can be found in Table 1.

#### 2.5. Synthesis of Nanostructured Titanium Sub-Oxides

It has become increasingly important to synthesize nanostructured titanium sub-oxides because of their particular properties resulting from the high surface areas of the materials. Nanostructured non-stoichiometric  $\text{TiO}_{2-x}$  titanium sub-oxides, titanium sub-oxides  $\text{Ti}_n\text{O}_{2n-1}$  in particular, have emerged as alternatives to  $\text{TiO}_2$  in applications of clean energy generation, and as catalysts for degrading harmful compounds and others [47–52]. Although titanium sub-oxides can be synthesized by the reduction of  $\text{TiO}_2$  using hydrogen or carbon, the sizes of synthesized titanium sub-oxide particles are usually in the order of micrometers, because these reduction reactions occur at high temperatures (generally over  $1000\text{ }^\circ\text{C}$ ) and proceed for hours. Under these conditions,  $\text{TiO}_2$  and formed titanium sub-oxide particles undergo sintering and crystal growth, leading to the formation of much larger particles. To synthesize nanostructured titanium sub-oxides, more reactive titanium-containing starting materials, stronger reducing agents or alternative reaction techniques are required for the reduction reactions to be carried out under milder reaction conditions such as lower temperatures or short reaction times.

Han et al. prepared  $\text{Ti}_8\text{O}_{15}$  nanowires and  $\text{Ti}_4\text{O}_7$  fibers by heating  $\text{H}_2\text{Ti}_3\text{O}_7$  nanowires in hydrogen at  $850\text{ }^\circ\text{C}$  and  $1050\text{ }^\circ\text{C}$  [53]. Hydrogen trititanate  $\text{H}_2\text{Ti}_3\text{O}_7$  is one of the compounds in the series of titanates ( $\text{M}_2\text{Ti}_n\text{O}_{2n+1}$ ,  $\text{M} = \text{H, Na, or K}$ ). The synthesis process has two steps. Firstly,  $\text{H}_2\text{Ti}_3\text{O}_7$  nanowires are prepared by reacting  $\text{TiO}_2$  particles with  $\text{NaOH}$  in an autoclave at  $150\text{--}180\text{ }^\circ\text{C}$  for 2–5 days, and then purified using the acid washing method [54–56]. Scanning electron microscopy (SEM) and transmission electron microscopy (TEM) studies showed that prepared  $\text{H}_2\text{Ti}_3\text{O}_7$  were nanowires of 30–200 nm in diameter and up to 10  $\mu\text{m}$  long. Secondly, prepared  $\text{H}_2\text{Ti}_3\text{O}_7$  nanowires were reduced in hydrogen for 1–4 h at  $800\text{--}1050\text{ }^\circ\text{C}$ . In the hydrogen reduction reaction at  $850\text{ }^\circ\text{C}$ ,  $\text{H}_2\text{Ti}_3\text{O}_7$  nanowires changed into  $\text{Ti}_8\text{O}_{15}$  nanorods or nanoparticles, as shown in Figure 2. By heating  $\text{H}_2\text{Ti}_3\text{O}_7$  in hydrogen at  $1050\text{ }^\circ\text{C}$ , the product formed was  $\text{Ti}_4\text{O}_7$ . The TEM image shows that most products are in the form of fibers, with diameters of approximately 1  $\mu\text{m}$ .

He et al. fabricated  $\text{Ti}_8\text{O}_{15}$  nanowires using an evaporation–deposition synthesis method [15]. The synthesized  $\text{Ti}_8\text{O}_{15}$  nanowires were  $\sim 30\text{ nm}$  in diameter (as shown in Figure 3), and were found to have an electrical conductivity of  $20.6\text{ S cm}^{-1}$ .

Zhang et al. prepared pure  $\text{Ti}_4\text{O}_7$  particles with diameters of 200–500 nm in hydrogen at  $850\text{ }^\circ\text{C}$  using peroxotitanium acid  $\text{H}_4\text{TiO}_5$  ( $\text{Ti}(\text{OH})_3\text{O-O-H}$ ) as a starting material [57].  $\text{H}_4\text{TiO}_5$  was prepared by treating titanium powder with  $\text{NH}_3\cdot\text{H}_2\text{O}$  and  $\text{H}_2\text{O}_2$ . Pang et al. synthesized  $\text{Ti}_4\text{O}_7$ , using a simple polymer-mediated route in which the cross-linked titanium ethoxide with polyethylene glycol was treated by carbothermal reduction at  $\sim 950\text{ }^\circ\text{C}$  in an Ar stream. TEM images revealed that the material primarily comprises  $\sim 8\text{--}20\text{ nm}$   $\text{Ti}_4\text{O}_7$  crystals. The sulfur composites  $\text{Ti}_4\text{O}_7/\text{S-60}$  or  $\text{Ti}_4\text{O}_7/\text{S-70}$  were prepared with either 60 or 70 wt% sulfur using a melt-diffusion method at  $155\text{ }^\circ\text{C}$  [58].  $\text{Ti}_4\text{O}_7$  was used to prepare  $\text{Ti}_4\text{O}_7/\text{S}$  cathodes for lithium–sulfur cells [59–61].

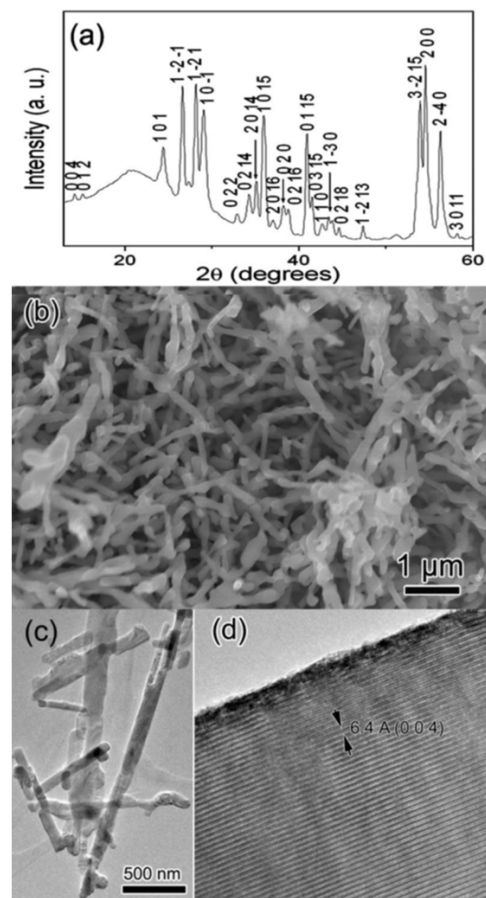


**Figure 2.**  $\text{Ti}_8\text{O}_{15}$  nanorods prepared by reducing  $\text{H}_2\text{Ti}_3\text{O}_7$  at  $850^\circ\text{C}$  in hydrogen; (a) XRD pattern of the product; (b) SEM image of the product; (c) low magnification TEM image of the product; and (d) a high-magnification TEM image of part of a nanorod (Reprinted from ref. [53], copyright 2008, American Institute of Physics).

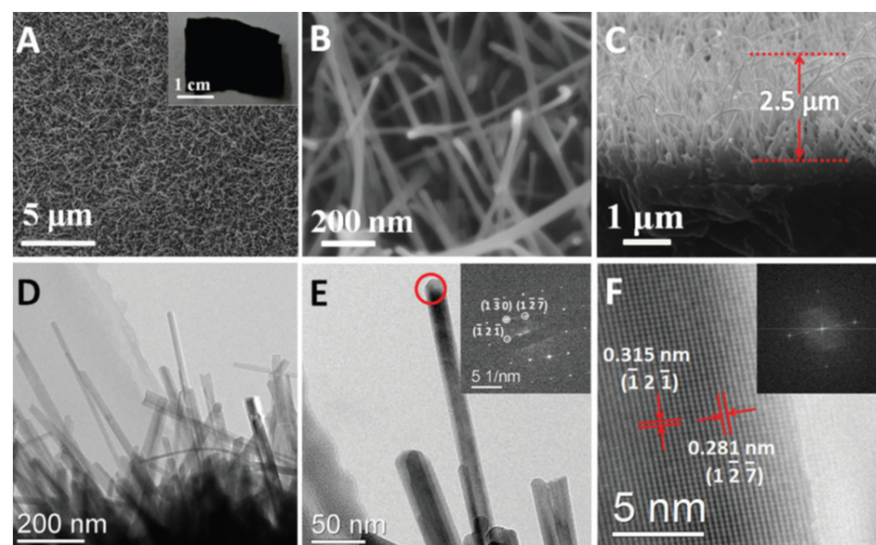


**Figure 3.** (A,B) SEM images of the  $\text{Ti}_8\text{O}_{15}$  nanowires; (C) SEM image of the cross-section of the  $\text{Ti}_8\text{O}_{15}$  nanowires; (D,E) TEM images of the  $\text{Ti}_8\text{O}_{15}$  nanowires; (F) HRTEM image of  $\text{Ti}_8\text{O}_{15}$  nanowires (Reprinted from ref. [15], copyright 2015, The Royal Society of Chemistry).

Portehault et al. developed a new bottom-up approach to synthesize various nano-scaled Magnéli phases under mild conditions [41]. In this method, titanium (IV) ethoxide was reacted with amino- or ethoxy-containing oligomers or polymers. The resulting clear gels were heated at different temperatures under  $N_2$  or Ar.  $Ti_nO_{2n-1}$  compounds ( $n = 3, 4, 5, 6, 8$ ) were obtained for the first time as nano-Magnéli phases with specific surface areas from  $55$  to  $300\text{ m}^2\text{ g}^{-1}$ . The synthesis steps for the Magnéli/carbon nanocomposites are illustrated in Figure 4.

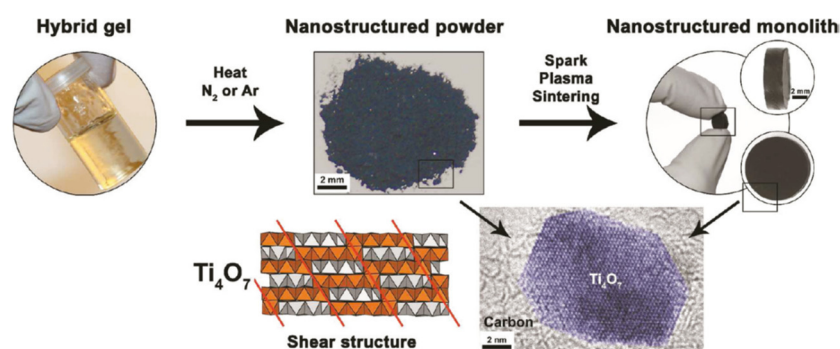


**Figure 4.** Synthesis steps for Magnéli/carbon nanocomposites (Reprinted from ref. [41], copyright 2011, American Chemical Society).

Huang et al. synthesized nanocrystalline  $Ti_2O_3$ ,  $Ti_3O_5$  and  $Ti_4O_7$  using a synthesis method that combines sol-gel and vacuum-carbothermic processes [44]. Yao et al. successfully synthesized  $Ti_4O_7$  using  $TiO(NO_3)_2$  as a starting material in a hydrogen atmosphere at  $1000\text{ }^\circ\text{C}$  for 6 h [22]. The SEM images clearly showed that the synthesized titanium sub-oxides are spherical particles with an average particle size of approximately 250 nm. Davydov synthesized  $Ti_4O_7$  nanopowder with an average size of  $115 \pm 30\text{ nm}$  using a two-step procedure. In the first step, titanium (III) oxalate particles with controlled sizes were produced by reacting metallic Ti with oxalic acid in a heated aqueous solution. In the second step,  $Ti_4O_7$  was prepared through high-temperature calcination of titanium (III) oxalate particles in a flowing hydrogen gas [62]. This synthesis process is similar to the process that has been used to prepare titanium oxycarbide nanoparticles [63]. Tominaka et al. synthesized  $Ti_2O_3$  nanoparticles by heating  $TiO_2$  nanoparticles (10–30 nm) and  $CaH_2$  powder at  $350\text{ }^\circ\text{C}$  [35].

Irooi et al. synthesized nanoparticles of titanium sub-oxides by irradiating  $TiO_2$  particles dispersed in liquid with a pulsed UV laser [64]. Xu et al. developed a synthesis process to prepare titanium sub-oxide nanoparticles via a thermal plasma method, using metatitanic acid  $H_2TiO_3$  ( $TiO(OH)_2$ ) as a starting material. The prepared titanium sub-oxides nanoparticles are spherical, with particle sizes in the range of 20–100 nm [23]. Fukushima et al. synthesized  $Ti_4O_7$  nanoparticles with different sizes by carbothermal reduction using a multimode microwave apparatus [28]. Takeuchi et al. synthesized 60 nm  $Ti_4O_7$  nanoparticles via carbothermal reduction of  $TiO_2$  nanoparticles using polyvinylpyrrolidone as the carbon source. The carbothermal reduction was carried out using 2.45 GHz microwave irradiation at  $950\text{ }^\circ\text{C}$  for 30 min. The results of this study demonstrate that microwave heating can drastically reduce the heating time to avoid excessive sintering and crystal growth of  $Ti_4O_7$  in a conventional carbothermal reduction process [65]. Arif et al. prepared chain-structured titanium sub-oxides with diameters under 30 nm using a thermal-induced plasma process. The synthesized titanium sub-oxide nanoparticles consisted of a mixture of several Magnéli phases. After a heat treatment, as-synthesized titanium sub-oxides nanoparticles were found to have low electrical resistivity [66].

A summary of synthetic methods for nanostructured titanium sub-oxides is reported in Table 2. A comparison among the synthesis methods to highlight the advantages, limitations and characteristics of the prepared sub-oxides is presented in Table 3.

**Table 2.** A summary of methods for synthesis of nanostructured titanium sub-oxides.

Materials	Method	Ref.
Ti <sub>8</sub> O <sub>15</sub> nanowires	Heating H <sub>2</sub> Ti <sub>3</sub> O <sub>7</sub> nanowires in hydrogen at 850 °C	[53]
Ti <sub>8</sub> O <sub>15</sub> nanowires	An evaporation–deposition synthesis method	[15]
Ti <sub>4</sub> O <sub>7</sub> particles with diameters of 200–500 nm	Reduction of H <sub>4</sub> TiO <sub>5</sub> with hydrogen at 850 °C	[57]
Ti <sub>4</sub> O <sub>7</sub> crystals (8–20 nm)	Carbothermal reduction of cross-linked titanium ethoxide with polyethylene glycol at ~950 °C in Ar stream	[58]
Magnéli phases with specific surface areas from 55 to 300 m <sup>2</sup> g <sup>−1</sup>	The gels made from titanium (IV) ethoxide and amino- or ethoxy-containing oligomers or polymers were heated at different temperatures under N <sub>2</sub> or Ar	[41]
Nanocrystalline Ti <sub>2</sub> O <sub>3</sub> , Ti <sub>3</sub> O <sub>5</sub> and Ti <sub>4</sub> O <sub>7</sub>	A combined sol-gel and vacuum-carbothermic processes	[44]
Ti <sub>4</sub> O <sub>7</sub> particles (around 250 nm)	Reduction of TiO(NO <sub>3</sub> ) <sub>2</sub> in hydrogen at 1000 °C for 6 h	[22]
Ti <sub>4</sub> O <sub>7</sub> nanopowder (115 ± 30 nm)	Reduction of titanium (III) oxalate particles in hydrogen	[62]
Ti <sub>2</sub> O <sub>3</sub> nanoparticles	Heating TiO <sub>2</sub> nanoparticles (10–30 nm) and CaH <sub>2</sub> powder at 350 °C	[35]
Titanium sub-oxide nanoparticles	Irradiation of TiO <sub>2</sub> particles dispersed in liquid with a pulsed UV laser	[64]
Titanium sub-oxide nanoparticles (20–100 nm)	By a thermal plasma method, using metatitanic acid (H <sub>2</sub> TiO <sub>3</sub> ) as a starting material	[23]
Ti <sub>4</sub> O <sub>7</sub> nanoparticles	Carbothermal reduction using a multimode microwave apparatus	[28]
Ti <sub>4</sub> O <sub>7</sub> nanoparticles (60 nm)	Carbothermal reduction of TiO <sub>2</sub> nanoparticles using microwave irradiation at 950 °C for 30 min	[65]
Titanium sub-oxides (30 nm)	A thermal-induced plasma process	[66]

**Table 3.** A comparative table among the synthesis methods.

Synthesis Methods	Advantages/Limitations	Characteristics
Hydrogen reduction	A simple, well established/handling reactive gas	For synthesis of multi-dimensional pure titanium sub-oxides
Carbon reduction	Use of various of carbon sources/uniform mixing of the reactants	For synthesis of various titanium sub-oxides by controlling mole ratio of carbon and TiO <sub>2</sub>
Metal reduction	Without handling reactive gas/controlling reaction process	Usually a mixture of different titanium sub-oxides
Hydride reduction	Reaction at relatively low temperature/handling reactive starting reactant	For synthesis of titanium sub-oxides with smaller particle sizes

### 3. Applications of Titanium Sub-Oxides

The structures of Magnéli phase titanium oxides are based on the rutile TiO<sub>2</sub> crystal lattice. Rutile TiO<sub>2</sub> is made up of octahedra having a titanium atom in the center and oxygen atoms at each corner. Shared edge or corner oxygen atoms link adjacent octahedra, as shown in Figure 5. The crystal structure of titanium sub-oxides can be described as a structure having a two-dimensional chain of titanium dioxide in which titanium atoms locate at the center and oxygen atoms locate at the corners in an octahedral structure [67,68]. In Ti<sub>n</sub>O<sub>2n−1</sub>, every nth layer has an oxygen deficiency, which leads to shear planes in the crystal structure. The Ti<sub>4</sub>O<sub>7</sub> crystal has three octahedral TiO<sub>2</sub> layers and one TiO layer. As a result of the vacancy of oxygen atoms, the TiO layer causes titanium atoms to be closer together.

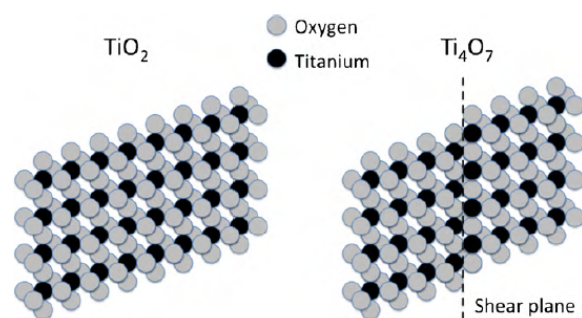


**Figure 5.** Edge-sharing  $\text{TiO}_2$  and  $\text{Ti}_4\text{O}_7$  octahedra sheets showing the face-sharing shear plane in  $\text{Ti}_4\text{O}_7$  (Reprinted from ref. [68], copyright 2010, Elsevier).

The unique crystal structure makes titanium sub-oxide materials have attractive properties, such as high conductivity, superior chemical stability and electrochemical stability [69]. As shown in Table 4, the conductivity of  $\text{Ti}_4\text{O}_7$  material is the highest among the Magnéli phase materials. Research shows that  $\text{Ti}_4\text{O}_7$  is highly stable in acidic or alkali conditions. Some studies indicated that the expected half-life of  $\text{Ti}_4\text{O}_7$  is 50 years in 1.0 M  $\text{H}_2\text{SO}_4$  at room temperature [70].

**Table 4.** Electrical conductivity for single Magnéli phase materials \*.

$\text{Ti}_n\text{O}_{2n-1}$ Phase	Electrical Conductivity ( $\sigma/\text{S cm}^{-1}$ )	Log10 ( $\sigma/\text{S cm}^{-1}$ )
$\text{Ti}_4\text{O}_7$	1995	3.3
$\text{Ti}_5\text{O}_9$	631	2.8
$\text{Ti}_6\text{O}_{11}$	63	1.8
$\text{Ti}_8\text{O}_{15}$	25	1.4

\* Adopted from ref. [68], copyright 2010, Elsevier.

As a result of their remarkable electrical conductivity, electrochemical stability, cost-effectiveness and environmentally friendly natures, titanium sub-oxides are also considered to have potential as a superior anode material for wider electrochemical applications [67,68]. Research has shown that Magnéli phases have a catalytic property. Among the Magnéli phases,  $\text{Ti}_4\text{O}_7$  exhibits the greatest catalytic property [45,69]. It has a wide electrochemical window with regard to water oxidation and reduction [70–72]; thus, it can be used for electrochemical treatment of pollutants in water. Titanium sub-oxides are generally prepared in the form of powders. More recently, two-dimensional films and three-dimensional porous materials of titanium sub-oxides have been successfully fabricated. Advances in the development of multiple dimensional titanium sub-oxide materials has led to new applications.

### 3.1. Catalysis Support in Fuel Cells

Proton exchange membrane fuel cells (PEMFCs) are a clean energy technology that has made significant advances in recent decades [73,74]. However, the high cost of the component materials and the low stability of the electrodes are major barriers for their large-scale commercial applications in some areas [75]. PEMFCs use Pt catalysts in the form of nanoparticles dispersed on a support material. The nature of the support materials can have a significant influence on the electro-activity and durability of the Pt catalysts [76–78]. Carbon materials are the most common support material for PEMFCs. However, carbon-supported Pt catalysts are prone to corrosion under the harsh operating conditions [79,80], which can severely affect the performance of PEMFCs and reduce the operational lifetime of the fuel cell electrodes. Titanium sub-oxides are considered to be promising support materials for PEMFCs due to the high thermal and oxidative stability, electronic conductivity and strong interactions between Pt nanoparticles and titanium sub-oxide support [81]. Chisaka et al. synthesized  $\text{Ti}_4\text{O}_7$  particles via carbothermal reduction, using titanium oxysulfate

(TiOSO<sub>4</sub>) and polyethylene glycol as precursors. The Pt catalyst using Ti<sub>4</sub>O<sub>7</sub> as support exhibited excellent load cycle durability, which was the highest among the state-of-the-art platinum/oxide catalysts, with no change in the cell performance after 10,000 voltage cycles [82]. Esfahani et al. synthesized doped titanium sub-oxide Ti<sub>3</sub>O<sub>5</sub>Mo<sub>0.2</sub>Si<sub>0.4</sub> (TOMS) as a novel fuel cell catalyst support. Ti<sub>3</sub>O<sub>5</sub>Mo<sub>0.2</sub>Si<sub>0.4</sub> (TOMS) support exhibited remarkably high electronic conductivity and high stability. The fuel cell devices that used the Pt/TOMS catalyst achieved high performance, better than that of commercial catalysts [83]. Nguyen et al. demonstrated the excellent durability of titanium sub-oxide as a catalyst support for Pd in alkaline direct ethanol fuel cells [84]. Won et al. developed Ti<sub>4</sub>O<sub>7</sub>-supported Pt-based catalysts for a bifunctional oxygen catalyst in a unitized regenerative fuel cell for both the oxygen reduction reaction (ORR) and the oxygen evolution reaction (OER) to enhance their activity and stability [85]. Zhang et al. developed an ordered Ag@Pd alloy supported on Ti<sub>4</sub>O<sub>7</sub>. The ordered characteristics of the Ag@Pd alloy and its strong electron transfer with the corrosion-resistant Ti<sub>4</sub>O<sub>7</sub> improved the catalytic activity and stability [86].

### 3.2. Electrocatalytic Degradation for Wastewater Treatment

Titanium sub-oxides have been characterized as an ideal choice of anode for the electrochemical treatment of many pollutants. Chen et al. decomposed trichloroethylene (TCE) and chloroform (CF) in an electrochemical cell using a titanium sub-oxide ceramic sheet plated with Pt or Pd as the working electrode. The decomposition kinetics was found to be of the first order for TCE and CF [87]. Kearney et al. used Ebonex (a titanium sub-oxide ceramic) electrodes for treating nitrate-contaminated water. Complete de-nitrification was achieved using an Ebonex cathode and a stable anode based on Ti/IrO<sub>2</sub> or Ti/RuO<sub>2</sub> [88]. Yang et al. examined the degradation of perfluorooctanesulfonate in electrochemical oxidation processes, using an anode made from Ti<sub>4</sub>O<sub>7</sub>. The decomposition rate of perfluorooctanesulfonate was shown to be pseudo-first-order. This study illustrates the promise of Ti<sub>4</sub>O<sub>7</sub> electrodes for degrading per- and polyfluoroalkyl compounds and co-contaminants in groundwater [89]. Ganiyu et al. reported a study of the electrochemical degradation of the antibiotic amoxicillin in aqueous solution. The Ti<sub>4</sub>O<sub>7</sub> anode of the cell was prepared using plasma spraying technology. The oxidative degradation of amoxicillin by hydroxyl radicals was assessed as a function of the applied current, and was found to follow pseudo-first-order kinetics. Comparative studies of mineralization efficiency showed that a Ti<sub>4</sub>O<sub>7</sub> anode performed better for the removal of total organic carbon (TOC) than the classical dimensional stable anode and Pt anode. Ti<sub>4</sub>O<sub>7</sub> anodes could provide a cost-effective alternative to boron doped diamond anodes in electro-oxidation processes [90]. Teng et al. investigated the electrochemical oxidation of sulfadiazine using a Ti/Ti<sub>4</sub>O<sub>7</sub> mesh anode. Their results showed that electrochemical oxidation could achieve almost 100% removal of sulfadiazine in 60 min under the conditions of 0.05 mol L<sup>-1</sup> Na<sub>2</sub>SO<sub>4</sub>, pH = 6.33 and current density of 10 mA cm<sup>-2</sup>. It was found that Ti/Ti<sub>4</sub>O<sub>7</sub> mesh anodes were very stable in the treatment of actual pharmaceutical wastewater, and had a large electrochemically active surface area due to the network structure of the Ti/Ti<sub>4</sub>O<sub>7</sub> mesh anode [91]. Further research will continue to improve the performance of titanium sub-oxide electrodes through optimizing the fabrication process of the electrodes and further integrating them with other technologies for more efficient applications.

### 3.3. Reactive Electrochemical Membrane

One recent research advancement in water treatment concerns the development of technologies that incorporate multiple treatment methods into a single technology to increase the efficiency and reduce the complexity of water treatment. A novel technology known as reactive electrochemical membranes (REM) combines membrane filtration with electrochemically advanced oxidation processes. In this REM technology, titanium sub-oxide materials serve as both a ceramic membrane for filtration and a reactive electrode surface for oxidizing contaminants [92]. Zaky et al. used Ti<sub>4</sub>O<sub>7</sub> REM to investigate the removal of p-substituted phenolic compounds in water. They demonstrated that the REM

was active for both direct anodic oxidation and production of  $\text{OH}\bullet$  radicals to degrade phenolic compounds [93]. Guo et al. synthesized a novel REMs for water treatment using tubular asymmetric  $\text{TiO}_2$  ultrafiltration membranes as precursors. REMs composed of high purity  $\text{Ti}_4\text{O}_7$  showed optimal reactivity. The performance of REMs was assessed by measuring the outer-sphere charge transfer ( $\text{Fe}(\text{CN})_6^{4-}$ ) and oxidation of organic compounds through both direct oxidation and generation of  $\text{OH}\bullet$ . In an optimal condition, the removal rate for oxalic acid was determined to be  $401.5 \pm 18.1 \text{ mmol h}^{-1} \text{ m}^{-2}$  at  $793 \text{ L m}^{-2} \text{ h}^{-1}$ . The current efficiency was approximately 84%. These results show the high promise of REMs in applications of water treatment [94]. Qi et al. prepared  $\text{Ti}_4\text{O}_7$  REM by thermal reduction of mechanically pressed  $\text{TiO}_2$  powders, using the Ti powder as the reducing agent. The prepared  $\text{Ti}_4\text{O}_7$  REMs show high oxygen evolution potential and electrocatalytic activity for the generation of  $\text{OH}\bullet$  [95]. You et al. fabricated a monolithic porous  $\text{Ti}_4\text{O}_7$  electrode for electrochemical oxidation of industrial dyeing and finishing wastewater. The electrochemical oxidation using porous  $\text{Ti}_4\text{O}_7$  electrode produced efficient and stable reduction of recalcitrant organic pollutants onsite, without any extra addition of chemicals [96]. Geng et al. fabricated tubular  $\text{Ti}_4\text{O}_7/\text{Al}_2\text{O}_3$  composite microfiltration membranes for electrically-assisted antifouling filtrations. The tubular  $\text{Ti}_4\text{O}_7/\text{Al}_2\text{O}_3$  membrane was tested for its antifouling performance by treating different feed solutions that are known to foul easily in an electrically-assisted membrane filtration module. The results demonstrated that the  $\text{Ti}_4\text{O}_7/\text{Al}_2\text{O}_3$  composite membranes showed much better antifouling performance than uncoated  $\text{Al}_2\text{O}_3$  membranes. The incorporation of a  $\text{Ti}_4\text{O}_7$ -modified membrane into the electrically-assisted filtration process provides a potential alternative for ceramic membrane filtrations to have antifouling properties for maintaining long-lasting permeate quality and simplifying the filtration operation [97]. Liang et al. developed a REM system using a  $\text{Ti}_4\text{O}_7$  microfiltration membrane as the filter and the anode. The REM system was evaluated for the performance in deactivating *Escherichia coli* (*E. coli*) in water at various current densities. The results showed that the concentration of *E. coli* was reduced from 6.46 log CFU/mL to 0.18 log CFU/mL, after passing through the  $\text{Ti}_4\text{O}_7$  microfiltration membrane filter. The scanning electron microscope and extracellular protein analysis showed that the membrane filtration effect and direct oxidation generated from the REM system are responsible for the observed bacteria removal and inactivation [98]. Research is continuing to optimize the electrode fabrication process, and to develop titanium sub-oxide electrodes doped with active electrode materials to further increase the efficiency of water treatment processes, prolonging electrode working life and expanding the degradation of complex pollutants.

### 3.4. Batteries

The lithium–sulfur battery (LSB) is considered to be one of the next-generation technologies for future batteries because of its remarkable specific capacity of  $1675 \text{ mA h g}^{-1}$  and the availability of low-cost sulfur [60,99]. However, the development of commercial LSBs needs to resolve the issues of low sulfur utilization and poor cyclability, which are caused by a number of factors, such as the low conductivity of sulfur, the high solubility of the lithium polysulfides, passivation of the reactive surface of lithium anodes, and so on. To address these issues, one of the research efforts is to develop host materials to limit the movement of the lithium polysulfides in the sulfur cathode. Tao et al. discovered that conductive  $\text{Ti}_4\text{O}_7$  was a highly effective matrix to bind with sulfur species.  $\text{Ti}_4\text{O}_7\text{-S}$  cathodes exhibit higher reversible capacity and improve cycling performance over previously developed  $\text{TiO}_2\text{-S}$  cathodes. The strong adsorption of sulfur species on the low-coordinated Ti sites of  $\text{Ti}_4\text{O}_7$  was attributed to the improved performance of  $\text{Ti}_4\text{O}_7\text{-S}$  cathodes [100]. Wei et al. prepared mesoporous  $\text{Ti}_4\text{O}_7$  microspheres that exhibit interconnected mesopores (20.4 nm), large pore volume ( $0.39 \text{ cm}^3 \text{ g}^{-1}$ ), and a high surface area ( $197.2 \text{ m}^2 \text{ g}^{-1}$ ). The sulfur cathode embedded with a matrix of mesoporous  $\text{Ti}_4\text{O}_7$  microspheres exhibits a superior reversible capacity and a low decay in capacity. The improved electrochemical performance is due to the strong chemical bonding of the lithium polysulfides to  $\text{Ti}_4\text{O}_7$ , and trapping in the mesopores and voids of the matrix [43]. Zhang et al. reported a facile

approach to prepare nanostructured  $\text{Ti}_4\text{O}_7$  with different morphologies.  $\text{Ti}_4\text{O}_7$  nanorods and nanoparticles were prepared. The as-prepared  $\text{Ti}_4\text{O}_7$  nanorods and nanoparticles were examined as a sulfur host for Li–S batteries. The electrochemical tests showed that the  $\text{Ti}_4\text{O}_7$  nanorods exhibited better performance in cycle stability and rate capacity compared with  $\text{Ti}_4\text{O}_7$  nanoparticles. This confirmed that the morphology of  $\text{Ti}_4\text{O}_7$  could influence its electrochemical performance for lithium sulfur batteries [101]. Wu et al. synthesized a composite containing carbon nanotubes and nanosized  $\text{Ti}_4\text{O}_7$  (oCNTs- $\text{Ti}_4\text{O}_7$ ), and coated the composite on the surface of the separator. Compared with a common separator, the separator modified with the oCNTs- $\text{Ti}_4\text{O}_7$  layer exhibited significantly improvement in the utilization of active substances, and restrained the shuttling effect of polysulfides. The Li–S battery fabricated using the separator modified with the oCNTs- $\text{Ti}_4\text{O}_7$  layer showed great enhancements in cycle and rate performance, as well as other in electrochemical properties [102]. Yu et al. fabricated a lithium–sulfur battery cathode containing 7.5 wt% to 10 wt%  $\text{Ti}_4\text{O}_7$ . The addition of  $\text{Ti}_4\text{O}_7$  as a conductive additive into the cathode resulted in better rate capability and reversible cycling performance. The high electronic conductivity and surface adsorption of the polysulfides of  $\text{Ti}_4\text{O}_7$  were attributed to the improvement in the electrochemical performance. This research also showed an effective way to improve the performance of lithium–sulfur batteries [103]. Titanium sub-oxides have also been used to improve the performance of other types of batteries such as lead–acid batteries and Zn–air batteries [104,105].

### 3.5. Other Applications

Titanium sub-oxides are also considered to be attractive for solar cells [106–110], sensors [111–115], electronic and photonic materials [3,7,16,116], and biological applications [117]. A summary of application areas of these materials in existing and emerging areas of research is listed in Table 5.

**Table 5.** Summary of application areas of Magnéli phases.

Area	Examples	Ref.
Electrodes	Electrodes for lead–acid batteries	[67]
Fuel cells	Conductive titanium sub-oxide support materials in fuel cells	[73–86]
Remediation of aqueous waste and contaminated water	Electrocatalytic degradation for wastewater treatment	[87–91]
$\text{Ti}_4\text{O}_7$ reactive membranes	Membranes for advanced electrochemical oxidation processes	[92–98]
Batteries	As a sulfur host in $\text{Li}_2\text{S}$ battery, and conductive additive for improving performance of $\text{Li}_2\text{S}$ battery	[43,60,99–105]
Solar cells	The $\text{TiO}/\text{TiO}_x$ layer can enhance the absorption of sunlight, thus increasing solar conversion efficiency	[106–110]
Sensors	Investigation of using nanostructured titanium sub-oxides as sensor materials for the determination of gaseous materials	[111–115]
Electronic and photonic materials	Nanostructured $\text{Ti}_4\text{O}_7$ in $\text{TiO}_2$ resistive switching memory. $\text{Ti}_3\text{O}_5$ for light-triggered metal semiconductor transition. Titanium sub-oxides as thermoelectric materials	[3,7,16,116]
Biological applications	Coating material for medical devices	[117]

#### 4. Summary and Outlook

In this review, recent progress in the synthesis and applications of Magnéli phase titanium oxides was reviewed. Titanium sub-oxides are synthesized through the reduction of titanium dioxide ( $\text{TiO}_2$ ) using hydrogen, carbon, metals or metal hydrides as reduction agents. The particle sizes of as-synthesized titanium sub-oxides are generally in the micrometer range, based on the conventional synthesis methods. However, progress has been made to synthesize nanostructured titanium sub-oxides through optimizing thermal reduction processes, using more powerful reduction agents or using new titanium-containing precursors [15,23,28,62,65,66]. Magnéli phase titanium oxides have numerous applications in electrodes, fuel cells, degradation of pollutants, batteries and coatings. Among these compounds,  $\text{Ti}_4\text{O}_7$  has received the most widespread attention due to its excellent electrical conductivity, and chemical and electrochemical stability. More recently, Magnéli phase titanium oxides as functional materials or additives have been used to enhance the performance of electro-catalysts, cathodes in batteries, advanced electrochemical oxidation processes, solar cells, electronic materials, sensors and coatings [95,110,111,118–122]. It is expected that further research will continue to optimize synthesis processes of Magnéli phase titanium oxides to further increase the electrochemical and catalytic properties, and to improve the performance of devices containing Magnéli phase titanium oxides through optimizing the fabrication process and further integrating with other technologies for more efficient applications. Titanium sub-oxides are expected to become more important materials for sustainability in the future.

**Author Contributions:** Conceptualization, X.W.; writing—original draft preparation, X.W. and H.W.; writing—review and editing, X.W., H.W. and Y.W.; project administration, Y.W.; funding acquisition, Y.W. All authors have read and agreed to the published version of the manuscript.

**Funding:** This research was financially supported by the National Natural Science Foundation of China (U19A20100).

**Institutional Review Board Statement:** Not applicable.

**Informed Consent Statement:** Not applicable.

**Data Availability Statement:** Not applicable.

**Acknowledgments:** Authors would like to thank R. Lu and Q. Miao for the technical assistance and administrative support in the preparation of the review.

**Conflicts of Interest:** The authors declare no conflict of interest.

#### References

1. Smith, J.R.; Walsh, F.C.; Clarke, R.L. Electrodes based on Magnéli phase titanium oxides: The properties and applications of Ebonex<sup>®</sup> materials. *J. Appl. Electrochem.* **1998**, *28*, 1021–1033. [[CrossRef](#)]
2. Li, X.; Zhu, A.L.; Qu, W.; Wang, H.; Hui, R.; Zhang, L.; Zhang, J. Magnéli phase  $\text{Ti}_4\text{O}_7$  electrode for oxygen reduction reaction and its implication for zinc-air rechargeable batteries. *Electrochim. Acta* **2010**, *55*, 5891–5898. [[CrossRef](#)]
3. Fan, Y.; Feng, X.; Zhou, W.; Murakami, S.; Kikuchi, K.; Normura, N.; Wang, L.; Jiang, W.; Kawasaki, A. Preparation of monophasic titanium sub-oxides of Magnéli phase with enhanced thermoelectric performance. *J. Eur. Ceram. Soc.* **2018**, *38*, 507–513. [[CrossRef](#)]
4. Kolbrecka, K.; Przulski, J. Sub-stoichiometric titanium oxides as ceramic electrodes for oxygen evolution-structural aspects of the voltammetric behaviour of  $\text{Ti}_n\text{O}_{2n-1}$ . *Electrochim. Acta* **1994**, *39*, 1591–1595. [[CrossRef](#)]
5. Inglis, A.D.; Page, Y.L.; Strobel, P.; Hurd, C.M. Electrical conductance of crystalline  $\text{Ti}_n\text{O}_{2n-1}$  for  $n = 4-9$ . *J. Phys. C Solid. State Phys.* **1983**, *16*, 317. [[CrossRef](#)]
6. Reyes-Coronado, D.; Rodr-guez-Gattorno, G.; Espinosa-Pesqueira, M.E.; Cab, C.; Coss, R.D.; Oskam, G. Phase-pure  $\text{TiO}_2$  nanoparticles: Anatase, brookite and rutile. *Nanotechnology* **2008**, *19*, 145605. [[CrossRef](#)]
7. Harada, S.; Tanaka, K.; Inui, H. Thermoelectric properties and crystallographic shear structures in titanium oxides of the Magnéli phases. *J. Appl. Phys.* **2010**, *108*, 083703. [[CrossRef](#)]
8. Ioroi, T.; Senoh, H.; Yamazaki, S.; Siroma, Z.; Fujiwara, N.; Yasuda, K. Stability of corrosion-resistant Magnéli-phase  $\text{Ti}_4\text{O}_7$ -supported PEMFC catalysts at high potentials. *J. Electrochem. Soc.* **2008**, *155*, B321–B326. [[CrossRef](#)]
9. Ehrlich, P. Phase Ratios and Magnetic Properties in the System Titanium-Oxygen. *Z. Elektrochem.* **1939**, *45*, 362.
10. Ehrlich, P. Lösungen von sauerstoff in metallischem titan. *Z. Anorg. Chem.* **1941**, *247*, 53–63. [[CrossRef](#)]

11. DeVries, R.C.; Roy, R. Phase diagram for the system Ti-TiO<sub>2</sub> constructed from data in the literature. *Am. Ceram. Soc. Bull.* **1954**, *33*, 370–372.
12. Andersson, S.; Collen, B.; Kuylenstierna, U.; Magnéli, A. Phase analysis studies on the titanium-oxygen system. *Acta Chem. Scand.* **1957**, *11*, 1641–1652. [[CrossRef](#)]
13. Bartholomew, R.F.; Frankl, D.R. Electrical properties of some titanium oxides. *Phys. Rev.* **1969**, *187*, 828. [[CrossRef](#)]
14. Jayashree, S.; Ashokkumar, M. Switchable intrinsic defect chemistry of titania for catalytic applications. *Catalysts* **2018**, *8*, 601. [[CrossRef](#)]
15. He, C.; Chang, S.; Huang, X.; Wang, Q.; Mei, A.; Shen, P. Direct synthesis of pure single-crystalline Magnéli phase Ti<sub>8</sub>O<sub>15</sub> nanowires as conductive carbon-free materials for Electrocatalysis. *Nanoscale* **2015**, *7*, 2856–2861. [[CrossRef](#)] [[PubMed](#)]
16. Kwon, D.H.; Kim, K.M.; Jang, J.H.; Jeon, J.M.; Lee, M.H.; Kim, G.H.; Li, X.S.; Park, G.S.; Lee, B.; Han, S.; et al. Atomic structure of conducting nanofilaments in TiO<sub>2</sub> resistive switching memory. *Nat. Nanotechnol.* **2010**, *5*, 148–153. [[CrossRef](#)]
17. Tsujimoto, Y. Low-temperature solid-state reduction approach to highly reduced titanium oxide nanocrystals. *J. Ceram. Soc. Jpn.* **2018**, *126*, 609–613. [[CrossRef](#)]
18. Yao, C.; Li, F.; Lia, X.; Xia, D. Fiber-like nanostructured Ti<sub>4</sub>O<sub>7</sub> used as durable fuel cell catalyst support in oxygen reduction catalysis. *J. Mater. Chem.* **2012**, *22*, 16560–16565. [[CrossRef](#)]
19. Geng, P.; Su, J.; Miles, C.; Comninellis, C.; Chen, G. Highly-ordered Magnéli Ti<sub>4</sub>O<sub>7</sub> nanotube arrays as effective anodic material for electro-oxidation. *Electrochim. Acta* **2015**, *153*, 316–324. [[CrossRef](#)]
20. Clarke, R.L. Conductive Titanium Suboxide Particulates. US5173215A, 22 December 1992.
21. Tang, C.; Zhou, D.; Zhang, Q. Synthesis and characterization of Magnéli phases: Reduction of TiO<sub>2</sub> in a decomposed NH<sub>3</sub> atmosphere. *Mater. Lett.* **2012**, *79*, 42–44. [[CrossRef](#)]
22. Yao, S.; Xue, S.; Zhang, Y.; Shen, X.; Qian, Y.; Li, T.; Xiao, K.; Qin, S.; Xiang, J. Synthesis, characterization, and electrochemical performance of spherical nanostructure of Magnéli phase Ti<sub>4</sub>O<sub>7</sub>. *J. Mater. Sci. Mater. Electron.* **2017**, *28*, 7264–7270. [[CrossRef](#)]
23. Xu, B.; Zhao, D.; Sohn, H.; Mohassab, Y.; Yang, B.; Lan, Y.; Yang, J. Flash synthesis of Magnéli phase (Ti<sub>n</sub>O<sub>2n-1</sub>) nanoparticles by thermal plasma treatment of H<sub>2</sub>TiO<sub>3</sub>. *Ceram. Int.* **2018**, *44*, 3929–3936. [[CrossRef](#)]
24. Kim, M.; Cho, N.; Kang, T.; Manh, N.; Lee, Y.; Park, K. Synthesis of highly conductive titanium suboxide support materials with superior electrochemical durability for proton exchange membrane fuel cells. *Mol. Cryst. Liq. Cryst.* **2020**, *707*, 110–117. [[CrossRef](#)]
25. Afir, A.; Achour, M.; Saoula, N. X-ray diffraction study of Ti-O-C system at high temperature and in a continuous vacuum. *J. Alloy. Compd.* **1999**, *288*, 124–140. [[CrossRef](#)]
26. Li, X.; Liu, Y.; Ye, J. Investigation of fabrication of Ti<sub>4</sub>O<sub>7</sub> by carbothermal reduction in argon atmosphere and vacuum. *J. Mater. Sci: Mater. Electron.* **2015**, *27*, 3683–3692. [[CrossRef](#)]
27. Toyoda, M.; Yano, T.; Tryba, B.; Mozia, S.; Tsumura, T.; Inagaki, M. Preparation of carbon-coated Magnéli phases Ti<sub>n</sub>O<sub>2n-1</sub> and their photocatalytic activity under visible light. *Appl. Catal. B Environ.* **2009**, *88*, 160–164. [[CrossRef](#)]
28. Fukushima, J.; Takizawa, H. Size Control of Ti<sub>4</sub>O<sub>7</sub> nanoparticles by carbothermal reduction using a multimode microwave furnace. *Crystals* **2018**, *8*, 444. [[CrossRef](#)]
29. Adamaki, V.; Clemens, F.; Ragulis, P.; Pennock, S.R.; Taylor, J.; Bowen, C.R. Manufacturing and characterization of Magnéli phase conductive fibres. *J. Mater. Chem. A* **2014**, *2*, 8328–8333. [[CrossRef](#)]
30. Acha, C.; Monteverde, M.; Nunez-Regueiro, M.; Kuhn, A.; Franc, M. Electrical resistivity of the Ti<sub>4</sub>O<sub>7</sub> Magnéli phase under high pressure. *Eur. Phys. J.* **2003**, *34*, 421–428. [[CrossRef](#)]
31. Gusev, A.; Avvakumov, E.; Vinokurova, O. Synthesis of Ti<sub>4</sub>O<sub>7</sub> Magneli phase using mechanical activation. *Sci. Sinter.* **2003**, *35*, 141–145. [[CrossRef](#)]
32. Hauf, C.; Kniep, R.; Pfaff, G. Preparation of various titanium suboxide by reduction of TiO<sub>2</sub> with silicon. *J. Mater. Sci.* **1999**, *34*, 1287–1292. [[CrossRef](#)]
33. Kitada, A.; Hasegawa, G.; Kobayashi, Y.; Kanamori, K.; Nakanishi, K.; Kageyama, H. Selective preparation of macroporous monoliths of conductive titanium oxides Ti<sub>n</sub>O<sub>2n-1</sub> (n = 2, 3, 4, 6). *J. Am. Chem. Soc.* **2012**, *134*, 10894–10898. [[CrossRef](#)] [[PubMed](#)]
34. Nagao, M.; Misu, S.; Hirayama, J.; Otomo, R.; Kamiya, Y. Magnéli-phase titanium suboxide nanocrystals as highly active catalysts for selective acetalization of furfural. *ACS Appl. Mater. Interfaces* **2020**, *12*, 2539–2547. [[CrossRef](#)] [[PubMed](#)]
35. Tominaka, S.; Tsujimoto, Y.; Matsushita, Y.; Yamaura, K. Synthesis of nanostructured reduced titanium oxide: Crystal structure transformation maintaining nanomorphology. *Angew. Chem. Int. Ed. Engl.* **2011**, *50*, 7418–7421. [[CrossRef](#)] [[PubMed](#)]
36. Kitada, A.; Kasahara, S.; Terashima, T.; Yoshimura, K.; Kobayashi, Y.; Kageyama, H. Highly reduced anatase TiO<sub>2-δ</sub> thin films obtained via low-temperature reduction. *Appl. Phys. Express* **2011**, *4*, 035801. [[CrossRef](#)]
37. Berger, L.M.; Gruner, W.; Langholf, E.; Stolle, S. On the mechanism of carbothermal reduction processes of TiO<sub>2</sub> and ZrO<sub>2</sub>. *Int. J. Refract. Met. Hard Mater.* **1999**, *17*, 235–243. [[CrossRef](#)]
38. Lekanova, T.L.; Ryabkov, Y.I.; Sevbo, O.A. Particle-size effect on the rate of carbon reduction of TiO<sub>2</sub>. *Inorg. Mater.* **2003**, *39*, 715–719. [[CrossRef](#)]
39. Maitre, A.; Tetard, D.; Lefort, P. Role of some technological parameters during carburizing titanium dioxide. *J. Eur. Ceram. Soc.* **2000**, *20*, 15–22. [[CrossRef](#)]
40. Dewan, M.A.; Zhang, G.; Ostrovski, O. Carbothermal reduction of titania in different gas atmospheres. *Metall. Mater. Trans.* **2009**, *40*, 62–69. [[CrossRef](#)]

41. Portehault, D.; Maneeratana, V.; Candolfi, C.; Deschler, N.; Veremchuk, I.; Grin, Y.; Sanchez, C.; Antonietti, M. Facile general route toward tunable Magnéli nanostructures and their use as thermoelectric metal oxide/carbon nanocomposites. *ACS Nano*. **2011**, *5*, 9052–9061. [[CrossRef](#)]
42. Mei, S.L.; Jafta, C.J.; Lauermann, I.; Ran, Q.; Kargell, M.; Ballauff, M.; Lu, Y. Porous Ti<sub>4</sub>O<sub>7</sub> particles with interconnected-pore structure as a high-efficiency polysulfide mediator for lithium-sulfur batteries. *Adv. Funct. Mater.* **2017**, *27*, 1701176. [[CrossRef](#)]
43. Wei, H.; Rodriguez, E.F.; Best, A.S.; Hollenkamp, A.F.; Chen, D.H.; Caruso, R.A. Chemical bonding and physical trapping of sulfur in mesoporous Magnéli Ti<sub>4</sub>O<sub>7</sub> microspheres for high-performance Li-S battery. *Adv. Energy Mater.* **2017**, *7*, 1601616. [[CrossRef](#)]
44. Huang, S.S.; Lin, Y.H.; Chuang, W.; Shao, P.S.; Chuang, C.H.; Lee, J.F.; Lu, M.L.; Weng, Y.T.; Wu, N.L. Synthesis of high-performance titanium sub-oxides for electrochemical applications using combination of sol-gel and vacuum-carbothermic processes. *ACS Sustain. Chem. Eng.* **2018**, *6*, 3162–3168. [[CrossRef](#)]
45. Strobel, P.; Le Page, Y. Crystal growth of Ti<sub>n</sub>O<sub>2n-1</sub> oxides (n = 2 to 9). *J. Mater. Sci.* **1982**, *17*, 2424–2430. [[CrossRef](#)]
46. Gusev, A.; Avvakumov, E.; Medvedev, A.; Masliy, A. Ceramic electrodes based on Magnéli phases of titanium oxides. *Sci. Sinter*. **2007**, *39*, 51–57. [[CrossRef](#)]
47. Fujishima, A.; Honda, K. Electrochemical photolysis of water at a semiconductor electrode. *Nature* **1972**, *238*, 37–38. [[CrossRef](#)]
48. Diebold, U. The surface science of titanium dioxide. *Surf. Sci. Rep.* **2003**, *48*, 53–229. [[CrossRef](#)]
49. Smestad, G.; Bignozzi, C.; Argazzi, R. Testing of dye sensitized TiO<sub>2</sub> solar cells I: Experimental photocurrent output and conversion efficiencies. *Sol. Energy Mater. Sol. Cells* **1994**, *32*, 259–272. [[CrossRef](#)]
50. Kay, A.; Grätzel, M. Low cost photovoltaic modules based on dye sensitized nanocrystalline titanium dioxide and carbon powder. *Sol. Energy Mater. Sol. Cells* **1996**, *44*, 99–117. [[CrossRef](#)]
51. Carp, O.; Huisman, C.L.; Reller, A. Photoinduced reactivity of titanium dioxide. *Prog. Solid. State Chem.* **2004**, *32*, 33–177. [[CrossRef](#)]
52. Konstantinou, I.K.; Albanis, T.A. TiO<sub>2</sub>-assisted photocatalytic degradation of azo dyes in aqueous solution: Kinetic and mechanistic investigations: A review. *Appl. Catal. B Environ.* **2004**, *49*, 1–14. [[CrossRef](#)]
53. Han, W.Q.; Zhang, Y. Magnéli phases Ti<sub>n</sub>O<sub>2n-1</sub> nanowires: Formation, optical, and transport properties. *Appl. Phys. Lett.* **2008**, *92*, 203117. [[CrossRef](#)]
54. Han, W.; Wu, L.; Klie, R.; Zhu, Y. Enhanced optical absorption induced by dense nanocavities inside titania nanorods. *Adv. Mater.* **2007**, *19*, 2525–2529. [[CrossRef](#)]
55. Kasuga, T.; Hiramatsu, M.; Hoson, A.; Sekino, T.; Niihara, K. Titania nanotubes prepared by chemical processing. *Adv. Mater.* **1999**, *15*, 1307–1311. [[CrossRef](#)]
56. Chen, Q.; Zhou, W.; Du, G.; Peng, L. Trititanate nanotubes made via a single alkali treatment. *Adv. Mater.* **2002**, *14*, 1208–1211. [[CrossRef](#)]
57. Zhang, X.; Liu, Y.; Ye, J.; Zhu, R. Fabrication and characterisation of Magnéli phase Ti<sub>4</sub>O<sub>7</sub> nanoparticles. *Micro Nano Lett.* **2013**, *8*, 251–253. [[CrossRef](#)]
58. Pang, Q.; Kundu, D.; Cuisinier, M.; Nazar, L. Surface-enhanced redox chemistry of polysulphides on a metallic and polar host for lithium-sulphur batteries. *Nat. Commun.* **2014**, *5*, 4759. [[CrossRef](#)] [[PubMed](#)]
59. Manthiram, A.; Fu, Y.; Su, Y. Challenges and prospects of lithium-sulfur batteries. *Acc. Chem. Res.* **2012**, *46*, 1125–1134. [[CrossRef](#)]
60. Evers, S.; Nazar, L.F. New approaches for high energy density lithium-sulfur battery cathodes. *Acc. Chem. Res.* **2013**, *46*, 1135–1143. [[CrossRef](#)]
61. Bresser, D.; Passerini, S.; Scrosati, B. Recent progress and remaining challenges in sulfur-based lithium secondary batteries—A review. *Chem. Commun.* **2013**, *49*, 10545–10562. [[CrossRef](#)]
62. Davydov, D.A. Preparation of nanostructured Ti<sub>4</sub>O<sub>7</sub>. *Inorg. Mater.* **2014**, *50*, 682–685. [[CrossRef](#)]
63. Davydov, D.A. Preparation of nanostructured Ti<sub>x</sub>O<sub>y</sub>. *Inorg. Mater.* **2013**, *49*, 62–65. [[CrossRef](#)]
64. Ioroi, T.; Kageyama, H.; Akita, T.; Yasuda, K. Formation of electro-conductive titanium oxide fine particles by pulsed UV laser irradiation. *Phys. Chem. Chem. Phys.* **2010**, *12*, 7529–7535. [[CrossRef](#)] [[PubMed](#)]
65. Takeuchi, T.; Fukushima, J.; Hayashi, Y.; Takizawa, H. Synthesis of Ti<sub>4</sub>O<sub>7</sub> nanoparticles by carbothermal reduction using microwave rapid heating. *Catalysts* **2017**, *7*, 65. [[CrossRef](#)]
66. Arif, F.; Balgis, R.; Ogi, T.; Iskandar, F.; Kinoshita, A.; Nakamura, K.; Okuyama, K. Highly conductive nano-sized Magnéli phases titanium oxide (TiO<sub>x</sub>). *Sci. Rep.* **2017**, *7*, 3646. [[CrossRef](#)] [[PubMed](#)]
67. Hayfield, P.C.S. *Development of a New Materials-Monolithic Ti<sub>4</sub>O<sub>7</sub> Ebonex<sup>®</sup> Ceramic*; Royal Society of Chemistry: Cambridge, UK, 2002.
68. Walsh, F.C.; Wills, R.G.A. The continuing development of Magnéli phase titanium sub-oxides and Ebonex (R) electrodes. *Electrochim. Acta* **2010**, *55*, 6342–6351. [[CrossRef](#)]
69. Pei, S.; Teng, J.; Ren, N.; You, S. Low-temperature removal of refractory organic pollutants by electrochemical oxidation: Role of interfacial joule heating effect. *Environ. Sci. Technol.* **2020**, *54*, 4573–4582. [[CrossRef](#)]
70. Nayak, S.; Chaplin, B.P. Fabrication and characterization of porous, conductive, monolithic Ti<sub>4</sub>O<sub>7</sub> electrodes. *Electrochim. Acta* **2018**, *263*, 299–310. [[CrossRef](#)]
71. Bunce, N.J.; Bejan, D. Pollutants in Water—Electrochemical remediation using Ebonex electrodes. In *Encyclopedia of Applied Electrochemistry*; Kreysa, G., Ota, K., Savinell, R.F., Eds.; Springer: New York, NY, USA, 2014; pp. 1629–1633. [[CrossRef](#)]

72. Liang, J.; You, S.; Yuan, Y.; Yuan, Y. A tubular electrode assembly reactor for enhanced electrochemical wastewater treatment with a Magnéli phase titanium suboxide (M-Ti<sub>2</sub>O<sub>3</sub>) anode and in situ utilization. *RSC Adv.* **2021**, *11*, 24976–24984. [[CrossRef](#)]
73. Debe, M.K. Electrocatalyst approaches and challenges for automotive fuel cells. *Nature* **2012**, *486*, 43–51. [[CrossRef](#)]
74. Jacobson, M.; Colella, W.; Golden, D. Cleaning the air and improving health with hydrogen fuel-cell vehicles. *Science* **2005**, *308*, 1901–1905. [[CrossRef](#)] [[PubMed](#)]
75. Service, R.F. Shrinking fuel cells promise power in your pocket. *Science* **2002**, *296*, 1222–1224. [[CrossRef](#)]
76. Borup, R.; Meyers, J.; Pivovar, B.; Kim, Y.S.; Mukundan, R.; Garland, N.; Myers, D.; Wilson, M.; Garzon, F.; Wood, D.; et al. Scientific aspects of polymer electrolyte fuel cell durability and degradation. *Chem. Rev.* **2007**, *107*, 3904–3951. [[CrossRef](#)] [[PubMed](#)]
77. Zhang, Z.; Liu, J.; Gu, J.; Su, L.; Cheng, L. An overview of metal oxide materials as electrocatalysts and supports for polymer electrolyte fuel cells. *Energy Environ. Sci.* **2014**, *7*, 2535–2558. [[CrossRef](#)]
78. Tian, Z.Q.; Lim, S.H.; Poh, C.K.; Tang, Z.; Xia, Z.; Luo, Z.; Shen, P.K.; Chua, D.; Feng, Y.P.; Shen, Z.; et al. A highly order-structured membrane electrode assembly with vertically aligned carbon nanotubes for ultra-low Pt loading PEM fuel cells. *Adv. Energy Mater.* **2011**, *1*, 1205–1214. [[CrossRef](#)]
79. Riese, A.; Banham, D.; Ye, S.; Sun, X. Accelerated stress testing by rotating disk electrode for carbon corrosion in fuel cell catalyst supports. *J. Electrochem. Soc.* **2015**, *162*, F783–F788. [[CrossRef](#)]
80. Prabhakaran, V.; Wang, G.; Parrondo, J.; Ramani, V. Contribution of electrocatalyst support to pem oxidative degradation in an operating PEFC. *J. Electrochem. Soc.* **2016**, *163*, F1611–F1617. [[CrossRef](#)]
81. Cherevko, S.; Kulyk, N.; Mayrhofer, K. Durability of platinum-based fuel cell electrocatalysts: Dissolution of bulk and nanoscale platinum. *Nano Energy* **2016**, *29*, 275–298. [[CrossRef](#)]
82. Chisaka, M.; Nagano, W.; Delgertsetseg, B.; Takeguchi, D. Inexpensive gram scale synthesis of porous Ti<sub>4</sub>O<sub>7</sub> for high performance polymer electrolyte fuel cell electrodes. *Chem. Commun.* **2021**, *57*, 12772–12775. [[CrossRef](#)]
83. Esfahani, R.; Ebraldize, I.; Specchia, S.; Easton, E. A fuel cell catalyst support based on doped titanium suboxides with enhanced conductivity, durability and fuel cell performance. *J. Mater. Chem. A* **2018**, *6*, 14805–14815. [[CrossRef](#)]
84. Nguyen, S.; Lee, J.; Yang, Y.; Wang, X. Excellent durability of substoichiometric titanium oxide as a catalyst support for Pd in alkaline direct ethanol fuel cells. *Ind. Eng. Chem. Res.* **2012**, *51*, 9966–9972. [[CrossRef](#)]
85. Won, J.; Kwak, D.; Han, S.; Park, H.; Park, J.; Ma, K.; Kim, D.; Park, K. PtIr/Ti<sub>4</sub>O<sub>7</sub> as a bifunctional electrocatalyst for improved oxygen reduction and oxygen evolution reactions. *J. Catal.* **2018**, *358*, 287–294. [[CrossRef](#)]
86. Zhang, L.; Luo, Y.; Huang, H.; Zhang, H.; Wang, Y.; Wang, Y. Ordered Ag@Pd alloy supported on Ti<sub>4</sub>O<sub>7</sub> by ascorbic acid-assisted galvanic replacement for efficient oxygen reduction. *J. Alloy. Compd.* **2022**, *929*, 167251. [[CrossRef](#)]
87. Chen, G.; Betterton, E.A.; Arnold, R.G.; Ela, W.P. Electrolytic reduction of trichloroethylene and chloroform at a Pt- or Pd-coated ceramic cathode. *J. Appl. Electrochem.* **2003**, *33*, 161–169. [[CrossRef](#)]
88. Kearney, D.; Bejan, D.; Bunce, N. The use of Ebonex electrodes for the electrochemical removal of nitrate ion from water. *Can. J. Chem.* **2012**, *90*, 666–674. [[CrossRef](#)]
89. Yang, P.; Wang, Y.; Lu, J.; Tishchenko, V.; Huang, Q. Electrochemical oxidation of perfluorooctanesulfonate by Magnéli phase Ti<sub>4</sub>O<sub>7</sub> electrode in the presence of trichloroethylene. *Adv. Environ. Eng. Res.* **2020**, *1*, 6. [[CrossRef](#)]
90. Ganiyu, S.O.; Oturan, N.; Raffy, S.; Cretin, M.; Esmilaire, R.; van Hullebusch, E.D.; Esposito, G.; Oturan, M.A. Sub-stoichiometric titanium oxide (Ti<sub>4</sub>O<sub>7</sub>) as a suitable ceramic anode for electro oxidation of organic pollutants: A case study of kinetics, mineralization and toxicity assessment of amoxicillin. *Water Res.* **2016**, *106*, 171–182. [[CrossRef](#)] [[PubMed](#)]
91. Teng, J.; Liu, G.; Liang, J.; You, S. Electrochemical oxidation of sulfadiazine with titanium suboxide mesh anode. *Electrochim. Acta* **2019**, *331*, 135441. [[CrossRef](#)]
92. Santos, M.C.; Elabd, Y.A.; Jing, Y.; Chaplin, B.P.; Fang, L. Highly porous Ti<sub>4</sub>O<sub>7</sub> reactive electrochemical water filtration membranes fabricated via electrospinning/electrospraying. *AIChE J.* **2016**, *62*, 508–524. [[CrossRef](#)]
93. Zaky, A.M.; Chaplin, B.P. Porous substoichiometric TiO<sub>2</sub> anodes as reactive electrochemical membranes for water treatment. *Environ. Sci. Technol.* **2013**, *47*, 6554–6563. [[CrossRef](#)]
94. Guo, L.; Jing, Y.; Chaplin, B.P. Development and characterization of ultrafiltration TiO<sub>2</sub> Magnéli phase reactive electrochemical membranes. *Environ. Sci. Technol.* **2016**, *50*, 1428–1436. [[CrossRef](#)]
95. Qi, G.; Wang, X.; Zhao, J.; Song, C.; Zhang, Y.; Ren, F.; Zhang, N. Fabrication and characterization of the porous Ti<sub>4</sub>O<sub>7</sub> reactive electrochemical membrane. *Front. Chem.* **2022**, *9*, 833024. [[CrossRef](#)] [[PubMed](#)]
96. You, S.; Liu, B.; Gao, Y.; Wang, Y.; Tang, C.; Huang, Y. Monolithic porous Magnéli-phase Ti<sub>4</sub>O<sub>7</sub> for electro-oxidation treatment of industrial wastewater. *Electrochim. Acta* **2016**, *214*, 326–335. [[CrossRef](#)]
97. Geng, P.; Chen, G. Magnéli Ti<sub>4</sub>O<sub>7</sub> modified ceramic membrane for electrically-assisted filtration with antifouling property. *J. Membr. Sci.* **2016**, *498*, 302–314. [[CrossRef](#)]
98. Liang, S.; Lin, H.; Habteselassie, M.; Huang, Q. Electrochemical inactivation of bacteria with a titanium sub-oxide reactive membrane. *Water Res.* **2018**, *145*, 172–180. [[CrossRef](#)] [[PubMed](#)]
99. Goodenough, J.B.; Park, K.S. The Li-ion rechargeable battery: A perspective. *J. Am. Chem. Soc.* **2013**, *135*, 1167–1176. [[CrossRef](#)]
100. Tao, X.; Wang, J.; Ying, Z.; Cai, Q.; Zheng, G.; Gan, Y.; Huang, H.; Xia, Y.; Liang, C.; Zhang, W.; et al. Strong sulfur binding with conducting Magnéli-phase Ti<sub>n</sub>O<sub>2n-1</sub> nanomaterials for improving lithium-sulfur batteries. *Nano Lett.* **2014**, *14*, 5288–5294. [[CrossRef](#)]

101. Zhang, Y.; Yao, S.; Zhuang, R.; Luan, K.; Qian, X.; Xiang, J.; Shen, X.; Li, T.; Xiao, K.; Qin, S. Shape-controlled synthesis of  $\text{Ti}_4\text{O}_7$  nanostructures under solvothermal-assisted heat treatment and its application in lithium-sulfur batteries. *J. Alloys Compd.* **2017**, *729*, 1136–1144. [[CrossRef](#)]
102. Wu, X.; Li, S.; Yao, S.; Liu, M.; Pang, S.; Shen, X.; Li, T.; Qin, S. Nanosized  $\text{Ti}_4\text{O}_7$  supported on carbon nanotubes composite modified separator for enhanced electrochemical properties of lithium sulfur battery. *Int. J. Energy Res.* **2021**, *45*, 4331–4344. [[CrossRef](#)]
103. Yu, C.; Tsai, C.  $\text{Ti}_4\text{O}_7$  as conductive additive in sulfur and graphene-sulfur cathodes for high-performance lithium-sulfur batteries with a facile preparation method. *MRS Energy Sustain.* **2022**, *9*, 369–377. [[CrossRef](#)]
104. Ellis, K.; Hill, A.; Hill, J.; Loyns, A.; Partington, T. The performance of Ebonex<sup>®</sup> electrodes in bipolar lead-acid batteries. *J. Power Sources* **2004**, *136*, 366–371. [[CrossRef](#)]
105. Huang, H.; Luo, Y.; Zhang, L.; Zhang, H.; Wang, Y. Cobalt-nickel alloys supported on  $\text{Ti}_4\text{O}_7$  and embedded in N, S doped carbon nanofibers as an efficient and stable bifunctional catalyst for Zn-air batteries. *J. Colloid. Interface Sci.* **2023**, *630*, 763–771. [[CrossRef](#)] [[PubMed](#)]
106. Roy, A.; Park, S.; Cowan, S.; Tong, M.; Cho, S.; Lee, K.; Heeger, A. Titanium suboxide as an optical spacer in polymer solar cells. *Appl. Phys. Lett.* **2009**, *95*, 013302. [[CrossRef](#)]
107. Lee, B.; Coughlin, J.; Kim, G.; Bazan, G.; Lee, K. Efficient solution-processed small-molecule solar cells with titanium suboxide as an electric adhesive layer. *Appl. Phys.* **2014**, *104*, 213305. [[CrossRef](#)]
108. Kim, S.; Park, S.; Lee, K. Efficiency enhancement in polymer optoelectronic devices by introducing titanium sub-oxide layer. *Curr. Appl. Phys.* **2010**, *10*, S528–S531. [[CrossRef](#)]
109. Arakawa, H.; Sayama, K.; Hara, K.; Sugihara, H.; Yamaguchi, T.; Yanagida, M.; Kawauchi, H.; Kashima, T.; Fujihashi, G.; Takano, S. Improvement of efficiency of dye-sensitized solar cell—Optimization of titanium oxide photoelectrode. In Proceedings of the 3rd World Conference on Photovoltaic Energy Conversion 2003, Osaka, Japan, 11–18 May 2003; Volume 1, pp. 19–22.
110. Kang, D.; Ko, J.; Lee, C.; Kim, C.; Lee, D.; Kang, H.; Lee, Y.; Lee, H. Titanium oxide nanomaterials as an electron-selective contact in silicon solar cells for photovoltaic devices. *Discov. Nano* **2023**, *18*, 39. [[CrossRef](#)]
111. Ramanavicius, S.; Ramanavicius, A. Insights in the application of stoichiometric and non-stoichiometric titanium oxides for the design of sensors for the determination of gases and VOCs ( $\text{TiO}_{2-x}$  and  $\text{Ti}_n\text{O}_{2n-1}$  vs.  $\text{TiO}_2$ ). *Sensors* **2020**, *20*, 6833. [[CrossRef](#)]
112. Ramanavicius, S.; Tereshchenko, A.; Karpicz, R.; Ratautaite, V.; Bubniene, U.; Maneikis, A.; Jagminas, A.; Ramanavicius, A.  $\text{TiO}_{2-x}/\text{TiO}_2$ -structure based ‘Self-Heated’ sensor for the determination of some reducing gases. *Sensors* **2019**, *20*, 74. [[CrossRef](#)]
113. Gardon, M.; Monereo, O.; Dosta, S.; Vescio, G.; Cirera, A.; Guilemany, J.M. New procedures for building-up the active layer of gas sensors on flexible polymers. *Surf. Coat. Technol.* **2013**, *235*, 848–852. [[CrossRef](#)]
114. Li, X.; Liu, Y.; Ma, S.; Ye, J.; Zhang, X.; Wang, G.; Qiu, Y. The synthesis and gas sensitivity of the  $\beta$ - $\text{Ti}_3\text{O}_5$  powder: Experimental and DFT study. *J. Alloy. Compd.* **2015**, *649*, 939–948. [[CrossRef](#)]
115. Lee, C.; Koo, S.; Oh, J.; Moon, K.; Lee, D. Selectable titanium-oxide-based critical and differential temperature sensor in a single devices. *IEEE Electron. Device Lett.* **2018**, *39*, 1058–1060. [[CrossRef](#)]
116. Ohkoshi, S.I.; Tsunobuchi, Y.; Matsuda, T.; Hashimoto, K.; Namai, A.; Hakoe, F.; Tokoro, H. Synthesis of a metal oxide with a room-temperature photoreversible phase transition. *Nat. Chem.* **2010**, *2*, 539–545. [[CrossRef](#)] [[PubMed](#)]
117. Bletsa, E.; Merkl, P.; Thersleff, T.; Normark, S.; Henriques-Normark, B.; Sotiriou, G. Highly durable photocatalytic titanium suboxide–polymer nanocomposite films with visible light-triggered antibiofilm activity. *Chem. Eng. J.* **2023**, *454*, 139971. [[CrossRef](#)]
118. Luo, Y.; Wang, Y.; Wang, Y.; Huang, H.; Zhang, L.; Zhang, H.; Wang, Y. Illumination enabling monoatomic Fe and Pt-based catalysts on NC/ $\text{TiO}_x$  for efficient and stable oxygen reduction. *Appl. Catal. B. Environ.* **2022**, *317*, 121797. [[CrossRef](#)]
119. Xiong, G.; Wang, Y.; Xu, F.; Tang, G.; Zhang, H.; Wang, F.; Wang, Y.  $\text{Au}(111)@\text{Ti}_6\text{O}_{11}$  heterostructure composites with enhanced synergistic effects as efficient electrocatalysts for the hydrogen evolution reaction. *Nanoscale* **2022**, *14*, 3878–3887. [[CrossRef](#)]
120. Wang, Y.; Zhao, D.; Zhang, K.; Li, Y.; Xu, B.; Liang, F.; Dai, Y.; Yao, Y. Enhancing the rate performance of high-capacity  $\text{LiNi}_{0.8}\text{Co}_{0.15}\text{Al}_{0.05}\text{O}_2$  cathode materials by using  $\text{Ti}_4\text{O}_7$  as a conductive additive. *J. Energy Storage* **2020**, *28*, 101182–101189. [[CrossRef](#)]
121. Liu, R.; Yang, L.; Wang, Y.; Liu, H.; Zhang, X.; Zeng, C. Effects of carbon nanotubes, graphene and titanium suboxides on electrochemical properties of  $\text{V}_2\text{Al}_{1-x}\text{CT}_z$  ceramic as an anode for lithium-ion batteries. *Ceram. Int.* **2021**, *47*, 35081–35088. [[CrossRef](#)]
122. Liu, H.; Xiao, H.; Qiao, Y.; Luo, M.; Wang, C.; Yang, L.; Zeng, C.; Fu, C. Preparation, characterization, and electrochemical behavior of a novel porous Magneli phase  $\text{Ti}_4\text{O}_7$ -coated Ti electrode. *Ceram. Int.* **2023**, *49*, 20564–20575. [[CrossRef](#)]

**Disclaimer/Publisher’s Note:** The statements, opinions and data contained in all publications are solely those of the individual author(s) and contributor(s) and not of MDPI and/or the editor(s). MDPI and/or the editor(s) disclaim responsibility for any injury to people or property resulting from any ideas, methods, instructions or products referred to in the content.